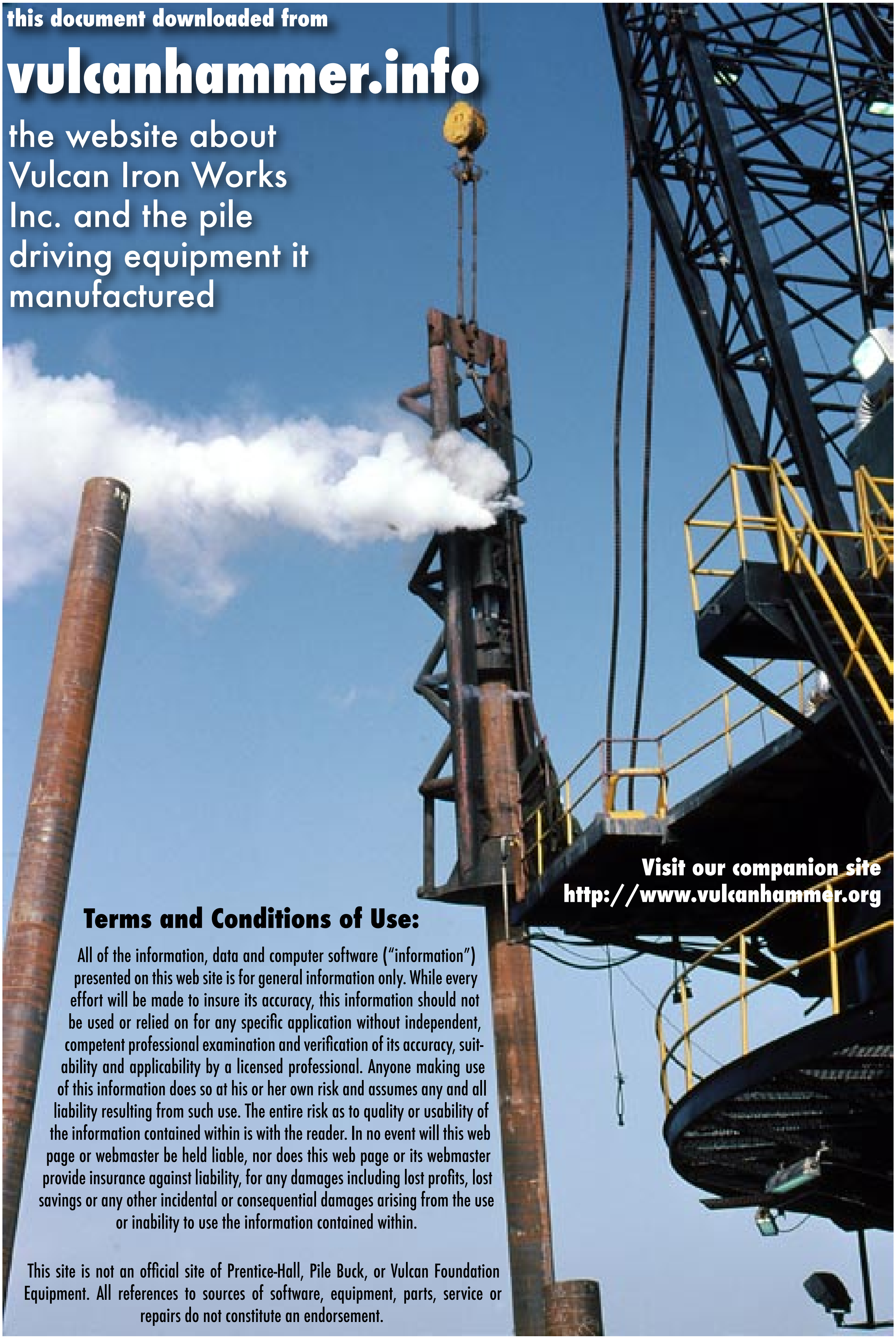

CHAPTER 23 Pile Driveability Analysis

Carl W. Fenske, P.E., Senior Geotechnical Consultant
McClelland Engineers, Inc., Houston, Texas

T. J. Hirsch, Ph.D., P.E., Professor of Civil Engineering
Texas A&M University, College Station, Texas

23.1 INTRODUCTION

The pile penetrations required to support the design loads for offshore structures are usually obtained from ultimate pile capacity curves developed by computations based on soil conditions as determined by a geotechnical investigation (see Chapter 21). When this procedure indicates large piles are to be installed to substantial penetrations or the soil conditions are such that the piles will have to penetrate dense sand layers or other strong soils, a question can arise whether the piles can be installed to the required penetration by driving only. Information to assist in answering this question may be developed by a pile drivability analysis.

The analysis of pile drivability consists of three phases or steps. The first step is to use an analysis based on the one-dimensional wave equation to estimate the resistance that can be overcome by the particular hammer-pile-soil system. The second step is to evaluate the specific soil conditions at the location to estimate the resistance that the soil will offer to the forced penetration of the pile. The third step is to compare the resistance the hammer-pile-soil system can overcome with the resistance that the soil can offer in order to obtain an indication whether the pile can be driven to the desired penetration. Engineers should be aware that a drivability analysis does not necessarily produce a definite answer to the pile drivability question. Considerable engineering judgement is required for all three steps of a drivability analysis, and everyone making a drivability analysis may not arrive at exactly the same conclusions. A drivability analysis should be made for each specific combination of hammer, pile and soil conditions being considered for a project.

23.2 WAVE EQUATION ANALYSIS

The impact of a pile driver ram on a pile can be represented for analytical purposes by the coaxial impact of a short rod and a long rod as shown by Fig 23.1(a). This ram impact results in a stress wave starting from the pile head and travelling down to the pile tip where it is reflected upward. This process continues until all energy in the force pulse is dissipated. The energy is dissipated by plastic soil deformation, soil damping, internal material damping in the pile, and other losses. The motion of the stress wave is described by the one-dimensional wave equation shown on Fig 23.1(b).

The idea of applying the wave equation to pile driving possibly was first suggested by D. V. Isaacs in 1931(1). A closed form analytical solution of the one-dimensional wave equation for a real hammer-pile-soil system is difficult if not impossible. In 1938, a solution attributed to E. N. Fox was published(2), but the simplifying assumptions necessary to achieve this solution reduced the value of the solution for a real pile driving problem.

In the 1950's, E. A. L. Smith[3][4][5] developed and proposed a step-by-step finite difference solution to the differential equation that could be used with the high-speed digital computers emerging at that time. This solution and the rapidly increasing availability of high-speed digital computers has led to the widespread use of the one-dimensional wave equation to analyze practical pile driving problems[6][7].

For a wave equation analysis, the pile driver ram, cushion, drive cap, pile and soil shown on the left side of Fig. 23-2 are modeled as shown on the right side. The ram is frequently represented by a concentrated mass, the cushion by a weightless spring, and the drive cap by a second point mass. The pile is divided into segments, each represented by a point mass equal to the mass of the segment and by a spring of stiffness equal to the stiffness of the segment.

Soil resistance is modeled by elastic-plastic springs and dashpots acting in parallel with the pile stiffness springs. The location and ultimate resistance of each of the soil springs is specified so as to represent the estimated distribution and total value of the soil resistance. The total soil resistance, R_u, is by definition the ultimate static soil resistance force acting on the pile during driving or immediately after driving is stopped. This ultimate static soil resistance during driving can be related to load bearing capacity by considering soil "set-up" after driving ceases. In the case of cohesionless soil, little if any set-up can normally be anticipated. In the case of cohesive soil, factors of 2 or 3 for set-up are not uncommon. The set-up factor is related to soil sensitivity and degree of remolding in friction.

The following paragraphs present a brief description of the step-by-step finite difference solution to the one-dimensional wave equation proposed by Smith[5] for single-acting steam/air hammers.

A value for the total soil resistance, R_u, is selected and this resistance is distributed on the side and tip of the embedded portion of the pile. Calculations begin when the ram contacts the hammer cushion. The ram is assigned an initial impact velocity which is based on the rated energy for the hammer, the weight of the ram and hammer efficiency; all other masses are usually assigned an initial velocity of zero. A time interval for iterative calculations is selected. Calculations describing the motions of the masses and the compressions of the springs are performed at times corresponding to the selected time intervals during the ram impact event. The interval to be used must be small relative to the shortest natural period of oscillation of adjacent spring-mass combinations within the system in order that the movements of the segments can be predicted accurately and that the calculations remain mathematically stable; for steel piles the time interval is frequently on the order of 1/5000 sec for a pile segment length of 8 to 10 ft.

For one time interval, a set of calculations is performed for each mass or segment, starting with the ram and proceeding to the pile tip. The calculations for each mass are as follows:

1. Calculate the new position of the mass by adding the initial position at the beginning of the time interval to the change in position which is the mass velocity multiplied by the time interval.

2. Calculate the compression and forces in all adjacent pile springs, soil springs and dashpots using the appropriate stiffness and damping coefficients.

3. Calculate the net force on the mass.

4. Calculate the acceleration of the mass as the force divided by the mass.

5. Calculate the new velocity for the mass by adding the product of the acceleration and time interval to the last velocity determined.

The calculation proceeds sequentially with the calculated motions and forces for the end of one time interval becoming the starting point for the calculations in the following interval. The process continues until the computed pile tip deflection reaches a maximum and begins to decrease, at which time the wave equation analysis for the assumed value of total soil resistance, R_u, is usually considered complete. Net pile penetration is usually calculated as the maximum gross movement of the pile tip less the elastic tip deflection. Net pile penetration is usually considered as the permanent set of the pile for the single blow. The inverse of the set per blow is the penetration rate, usually expressed in blows per inch, or blows per foot, for the initially selected value of ultimate static soil resistance, R_u. In normal practice, the above calculations are repeated for several values of R_u, and the results are summarized on a plot of R_u versus Penetration Rate (Blows Per Foot), called a bearing graph, as shown in Fig. 23-3. Fig. 23-3 shows that the maximum soil resistance that can be overcome by this hammer-pile-soil system is about 2900 kips and depends to some extent on the pile penetration. Because of the complex interrelation between parameters, it generally is not wise to attempt to extrapolate the effects of variation in a parameter from one hammer-pile-soil system to another. Consequently, a wave equation analysis should be performed for a specific hammer-pile-soil system using specific values for as many of the parameters as possible. Knowledge of the parameters for the wave equation analysis is important whether one is going to make the analysis or only furnish the specific parameter information for the analysis.

The input parameters for a wave equation analysis can be divided into three groups corresponding to the three parts of the hammer-pile-soil system. The following discussion of the principal parameters is directed primarily toward the system used predominantely in offshore construction, namely steam hammers and steel pipe piles.

Hammer Parameters. The pile driving hammer is described by (1) the rated hammer energy, (2) the weight of the ram or striking parts, (3) the efficiency of the hammer, (4) the weight of the drivehead or pile cap, (5) the capblock spring constant, and (6) the coefficients of restitution for the ram hitting the capblock and for the pile cap-pile contact. The rated energy and the ram weight are established by the make and model of the hammer and may be obtained from manufacturer's literature. Information for some hammers used for offshore pile driving is given in Table 23-1. The hammer efficiency, which relates the actual energy to the rated energy for the hammer, depends on the condition of the hammer and the operating procedure at the time of pile driving. Hammer efficiency can vary over a wide range and considerable experience or experimental data is needed to estimate it. Specific information on hammer efficiency usually is not available when a wave equation analysis is made but it can be obtained from measurements made in the field during driving (see Chapter 25). For hammers with a fixed ram stroke, the efficiency probably is not greater than about 90 percent even when in excellent condition and operated properly and can be 30 percent or less if the hammer is in poor condition or not operated properly because of insufficient steam pressure at the hammer. Efficiencies over 100 percent have been measured for hammers having a variable stroke operated at less than maximum stroke. This can be attributed for this type of hammer to overstroke when operated at a lower stroke setting. The hammer efficiency enters the wave equation analysis in the calculation of the velocity of impact of the ram on the pile:

$$v_i = \sqrt{2g(h)(e)} \tag{23.1}$$

where h = effective ram stroke (for double acting or diesel hammers the actual physical stroke is not the effective stroke), L

e = hammer efficiency

g = acceleration due to gravity, LT^{-2}

Since the velocity of impact for the ram is a function of the square root of the hammer efficiency, it is not sensitive to small changes in efficiency. Most wave equation analyses are made using hammer efficiencies of 60 to 70 percent unless there is specific knowledge of a more realistic value for a particular hammer.

The drive cap used with any type or model hammer can vary depending on the type and size of pile to be driven and on contractor preferences. Consequently, it is preferable that a wave equation analysis be made using specific information for the particular drive cap that is to be used to install the piles. The cushion used with a given hammer also is variable. The area and thickness of the cushion and the cushion material used is a function to some extent of the drive cap used but also may depend on contractor preferences.

The primary purpose of the cushioning material in the drive cap is to limit impact stresses in the pile and in the hammer. In doing this, however, a certain amount of the impact energy is absorbed in nonlinear deformation of the cushion material. In the idealization of the cushion material, the load-deformation behavior can be represented by two straight lines with different slopes as shown in Fig. 23-4. The slope of the loading line is called the spring constant of the capblock which can be calculated by:

$$k = AE/t \tag{23.2}$$

where k = spring constant of cushion, FL^{-1}

A = cross-sectional area of cushion, L^2

t = thickness of cushion, L

E = dynamic modulus of elasticity of cushion material, FL^{-2}

The slope of the unloading line is equal to the spring constant divided by the square of the coefficient of restitution. If the cushion in the drive cap consists of more than one material, then the spring constant of the cushion is obtained by:

$$\frac{1}{k} = \frac{1}{k_1} + \ldots\ldots \frac{1}{k_n} \tag{23.3}$$

where n = the number of cushioning materials in the capblock.

The values of k_1, etc. are computed using the dynamic modulus of elasticity, E, and the thickness, t, for each of the materials in the cushion. As for the drive cap weight, it is preferable that a wave equation analysis be made using information for the specific cushion that will be used. The specific information required is the area and thickness of the cushion and the dynamic modulus of elasticity and coefficient of restitution for the cushioning material. Dynamic modulus of elasticity and coefficient of restitution values for some typical cushion materials are given in Table 23.2; additional information on these cushion parameters is given in Chapter 25. For most offshore piles, the drive cap rests directly on the top of the pile. Because neither the drive cap nor the pile top are perfectly smooth, because the drive cap may not sit squarely on the pile top and because of the discontinuity, there will be some energy losses at this point during driving that can be approximated by using a coefficient of restitution of about 0.9.

Pile Parameters. The following information is required to define a pipe pile in a wave equation analysis: (1) pile diameter; (2) schedule of wall thickness variation and length of each wall thickness; (3) modulus of elasticity and unit weight of the pile material; and (4) lengths of the initial pile section and each add-on. For the idealized pile as shown on Fig. 23-2, the pile is divided into segments which should be approximately the same length. The segment length should be on the order of 8 to 10 ft for a steel pile. This means that the number of pile sections is proportional to the pile length. The step-by-step finite difference solution of the wave equation may become unstable if the segment length is made too long, while a shorter segment length just adds to the number of segments and thereby to the computing time.

An offshore pile usually has a considerable length above the soil surface. The position of the soil surface should be taken into account in dividing the pile into segments. The length of an offshore pile usually is increased in sections, or add-ons, as it is being driven. The pile for a wave equation analysis should include those sections that would be in place for a given pile penetration. The weight of the pile and the distribution of wall thicknesses can have a very significant effect in the maximum resistance that can be overcome by a given hammer-pile-soil system as determined by a wave equation analysis. Consequently, it is important for a drivability analysis that the pile used in the wave equation analysis is similar in make-up to the actual pile that will be driven.

Soil Parameters. The parameters in a wave equation analysis that are related to the soil include the following: (1) the elastic ground compression, commonly referred to as quake, on the sides and at the tip of the pile; (2) the damping constant on the side and at the tip of the pile; (3) the total static soil resistance to driving for the pile; and (4) the distribution of the total static soil resistance to driving between the side and the tip of the pile. For the idealized pile shown on Fig. 23-2, the first two parameters are represented by the spring and dashpot shown on the side of each element below ground line and at the pile tip. The load-deformation characteristics of the idealized soil spring is illustrated in Fig. 23-5(a). The spring can deform elastically to a maximum deformation, Q, after which there is no additional resistance from continued deformation. The value of Q is the quake which is the first soil parameter given above. The maximum static resistance for the side of each pile element and at the pile tip is obtained from the last two soil parameters listed above. With the maximum static resistance established, the spring constant for the soil spring at the side of each pile element and at the tip is given by:

$$k = R/Q \tag{23.4}$$

where k = soil spring constant, FL^{-1}

R = maximum static soil resistance at side of pile element or pile tip, F

Q = soil quake, L

The dashpot in parallel with the spring at the side of each element and at the pile tip is included to account for the dynamic, or velocity-related, effects on the soil characteristics. The total resistance of the soil spring and dashpot under dynamic load is illustrated on Fig. 23-5(b). The resistance of the dashpot is assumed to be directly proportional to the velocity of the associated segment during the displacement. Because of the direct proportionality to velocity, this resistance will be referred to here as linear viscous damping. The relation between the dynamic soil resistance at the side of a pile element or at the pile tip is given by:

$$R_d = R_s \{1 + J(V)\} \tag{23.5}$$

where R_d = dynamic soil resistance, F

R_s = static soil resistance, F

J = soil damping constant, TL^{-1}

V = velocity of the pile element, LT^{-1}

Information on the variation of values for soil quake, Q, and the soil damping, J, for various soil types and conditions is not extensive and is still the subject of much study. This information is generally obtained by full-scale pile load tests where the resistance during driving is measured by or extrapolated from the load test results. Wave equation analyses are made with varying values for quake and damping to determine those values which give the best agreement with the measured resistance to driving and the observed rate of penetration for the pile. A historical summary of quake and damping values is given in Table 23-3(5)(8)(9)(10)(11)(12). Values of damping presented in this table are for linear viscous damping as described above. Care must be used in selecting values of quake and damping from sources such as those used for Table 23.3. The quake and damping values from a given source should be used together because both values probably were used in their development from field tests. The values of quake and damping for each source on Table 23.3 depend to some extent on the soil and pile condition for which they were developed. For example, the values of quake and damping developed by Roussel(12) were from analyses of driving data for large, high-capacity offshore pipe piles in the Gulf of Mexico. Because the tip resistance for these piles is small relative to the side resistance, halving or doubling of the reported damping values at the tip probably would not have significantly affected the correlation. Consequently, the values for quake and damping proposed by Roussel may not be suitable for smaller, shorter piles, particularly where the resistance is primarily in end bearing.

Researchers are publishing laboratory test results(13) presenting soil damping values based on nonlinear damping not directly proportional to to velocity. Care should be taken in using these values because most computer programs would need modification to handle them properly. In addition, most of these nonlinear viscous damping values have not been correlated with load test results. Engineering judgement should be used to select values for quake and damping that are most appropriate for the pile and soil conditions being analyzed and the wave equation analysis computer program being used.

23.3 RESISTANCE TO DRIVING OFFERED BY SOIL

The second step in a drivability analysis is to estimate the resistance the soil will overcome when a pile is forced into the ground by blows from the driving hammer. The starting point for the estimation can be an ultimate pile capacity curve developed from a geotechnical investigation. Procedures for computing ultimate pile capacity[14][15] (also see Chap. 21) are semi-empirical in nature and are based on correlations with results from pile load tests made several days after the piles were installed. For many soils, particularly cohesive soils, the ultimate pile capacity several days after installation can be significantly greater than the ultimate capacity during driving and immediately after driving stops. This is illustrated by the load test results[16] shown on Fig. 23-6 which show measured increases in pile capacity with time for steel friction piles in cohesive soils. These results suggest that the ultimate capacity of a friction pile in clays is not obtained until a month or more after driving. There are other soils, generally cohesionless soils, that exhibit relatively little change in ultimate capacity with time after driving. One method to estimate the resistance offered by the soil during pile driving from the ultimate pile capacity some time after driving is to evaluate the effects of driving on the components of the static pile capacity which are the frictional resistance on the side and the end bearing on the tip of the pile.

Side Friction. The pile-soil static frictional resistance can change during driving and after driving has ceased. The magnitude of this change depends to some extent on the type of the soil. For piles in sand, the static resistance during driving usually is assumed to be equal to the static resistance several weeks after driving. There is some field evidence of this because when there is a significant delay in driving a pile in sand, the rate of penetration for the pile frequently is about the same after the delay as it was just before the delay.

For many clays, the static friction resistance during driving may be significantly less than the static friction resistance a few weeks or sometimes even hours, after driving. To illustrate this, consider Fig. 23-7 which shows typical in situ and remolded strength profiles for a normally-consolidated clay. During driving of a long offshore pile, the clay can be remolded almost completely during continuous driving. The reduction in frictional resistance at a given depth probably is a function of the length of pile that has passed that depth as suggested by the "friction fatigue" theory proposed by Heerema[17]. However, until there are proven methods to evaluate this, the static resistance during driving of long offshore piles in clays can be estimated by assuming the clays to be completely remolded. After driving ceases, the pile-soil frictional resistance for many clays increases until it approaches, after a few weeks, the static resistance as estimated by one of the computational procedures for ultimate pile capacity. This can produce the different pile capacities shown on Fig. 23-8. The ratio of the final capacity to the soil resistance during driving is called soil "set-up." Information from a limited number of tests on full-scale piles driven in clay indicates that the magnitude of the "set-up" may be on the order of the ratio of the undisturbed to the remolded soil shear strength, referred to as the sensitivity of the clay. This lends some credence to the use of the remolded shear strength of clays to estimate the friction resistance during driving in clays.

End Bearing. End bearing resistance to driving of a pile probably is related to the undisturbed shear strength of the soil, and unit end bearing resistance can be computed on this assumption. The primary variable in the end bearing resistance is the effective end area. For piles with solid cross-sections or with end closures, the effective end area is the gross end area. Most offshore piles, however, are steel pipes driven with open ends. In the initial driving, this pile type usually will "core" the soil so that the soil surface inside and outside the pile are at about the same level. The end bearing in this case is only on the cross-sectional end area of the pipe walls. When the pile is driven to greater penetrations or possibly when it encounters a stronger material such as sand or hard clay, the pile may "plug" so that the soil inside the pile moves with the pile as it moves downward. With the present state of the art, it is difficult to predict when a pile will plug, but it probably is true that a deep-penetrating pile will reach refusal to driving within a few feet after it plugs. During continuous driving in clay, large diameter pipe piles are not likely to plug. If driving ceases for several hours or days, however, a plug can form due to soil set-up.

It can be seen from the above discussion that there is no unique resistance during driving for a pile. We can, however, take the soil information and develop estimated resistance during driving for several conditions that could develop during the installation. Curve 1 on Fig. 23-9 is the estimated resistance during continuous driving. This curve is obtained by computing side friction in clays using remolded shear strengths, side friction in sands using the static side friction, and the end bearing on the pile wall end area (no plug). There is no reliable way to distinguish between the friction on the outside of the pile from that from the soil column inside the pile. The procedure for estimating side friction given above using the outside surface area of the pile is considered to represent the combined side-frictional resistance for the pile during continuous driving. Curve 2 on Fig. 23-9 is the estimated resistance during driving if the pile plugs so that the soil inside the pile moves downward with the pile. This curve is obtained by using the same side frictional resistance as for Curve 1 but with end bearing on the gross end area of the pile. Curve 3 on Fig. 23-9 is the computed ultimate compressive capacity for the pile and is an estimate of the resistance to driving after a long delay in the driving. Curves 1 and 3 on Fig. 23-9, therefore, represent the range of estimated resistance to driving that might be encountered in the installation of a pile by driving.

23.4 INTERPRETATION OF DRIVABILITY

The interpretation of drivability consists of comparing the resistance that can be overcome by a given hammer-soil-pile system to the resistance that the soil will offer to pile penetration. One method to interpret drivability is illustrated on Fig. 23-9. Curves 1, 2 and 3 represent the estimated resistance that the soil will offer to pile driving under different conditions and circumstances that might be encountered during the pile installation. Information on the resistance that can be overcome by the hammer-pile-soil system is presented on Fig. 23-3. Because of damage to the pile-driving hammer and other equipment with hard driving, most hammer manufacturers and consequently pile installation contractors will place a limit to the number of blows per foot of pile penetration at which they will continue to operate hammers for any great period of time. If the assumption is made that this limit is 200 blows per foot, values for the greatest resistance that can be overcome by the particular hammer-pile-soil system at different depths can be obtained by the intersection of the line for 200 blows per foot with the curves on Fig. 23-3. These values are plotted at the respective depths on Fig. 23-9 and are used to construct the dashed line representing the trend with pile penetration for the resistance that can be overcome by the hammer-pile-soil system used for the wave equation analysis. This trend line intersects Curve 3 at a penetration of about 210 ft and Curve 1 at a penetration of about 330 ft. This immediately indicates two factors concerning pile drivability. The first is that there should be no problem for this hammer to drive this pile at this location to a penetration of about 210 ft. The second fact is that even under the best circumstances it may not be possible to drive this pile with this hammer to a penetration more than about 330 ft. For pile penetrations between 210 and 330 ft, pile drivability is less definite because the penetration to which the pile can be driven may depend on factors that are not easily predictable.

One factor that is not easily predictable is plugging of the pile. There is very little information available at this time to predict with any certainty if a pile will plug during driving or the depth at which it might plug. The trend line intersects Curve 2 at a penetration of about 305 ft which indicates that it may not be possible to drive a pile below this penetration if the pile should plug. While the effect of the pile plugging on the penetration to which the pile can be driven is relatively minor for the hammer-pile-soil system of Fig. 23-9, the effect is more significant for the system shown on Fig. 23-10. The information on Fig. 23-10 would indicate that the pile would reach refusal almost immediately if it plugs after the tip enters the sand layer found at a penetration of about 240 ft.

A second factor that may not be predictable is the number and length of any delays during the pile installation. If there is a delay during driving, particularly if the pile is being driven in predominately clay as the case for Fig. 23-9, the resistance of the soil to the pile penetration will tend to increase from that indicated by Curve 1 towards the resistance indicated by Curve 3. As the penetration for the trend line for the greatest resistance that can be overcome by the hammer-pile-soil system increases below the intersection of the trend line and Curve 3 towards Curve 1, the penetration to which the pile can be driven becomes more susceptible to the length of any delay during driving. Long offshore piles are driven in sections and there are delays in driving as the sections are stabbed and welded onto the driven portion of the pile. These delays are necessary and while the number is known, the lengths are not. The information such as that presented on Fig. 23-9 and 23-10 may be used to plan the locations of the pile add-ons to minimize the effects of the necessary delays. This information also can be used to make an evaluation of the possible effects of unforeseen delays due to weather, equipment breakdowns and other causes.

A second method to interpret drivability is illustrated on Fig. 23-11 which presents three curves of estimated driving rate in blows per foot of penetration versus pile penetration. These curves were obtained from the estimated resistance to driving offered by the soil given in Fig. 23-9 and the resistance that can be overcome by the hammer-pile-soil system given in Fig. 23-3. The lower curve on Fig. 23-11 was developed by obtaining values for the estimated resistance offered by the soil at various penetrations from Curve 1 on Fig. 23-9 and using these values to obtain estimated driving rates at the penetrations from the curves on Fig. 23-3. The other two curves on Fig. 23-11 were developed in a similar manner using Curves 2 and 3 on Fig. 23-9.

The interpretation of drivability using information as presented on Fig. 23-11 is similar to the interpretation using information as presented on Fig. 23-9. Assuming that a driving rate of 200 blows per foot represents the driving limit, it may be seen on Fig. 23-11 that there should be no problem to drive the pile to a penetration of about 210 ft. It also can be seen that it may be difficult, even under the best conditions, to drive the pile to a penetration much greater than about 330 ft. In between these two depths, the penetration to which the pile can be driven will depend on whether the pile plugs, on the duration of any delays during driving and the penetration at which they occur, and on other factors that are not entirely predictable.

It should be evident from the information presented here that a drivability analysis does not necessarily produce a single or unique answer to the question about the ability of a given hammer to install a particular pile to a specific penetration at a location. It should be recognized that precise, singular results are not obtained from either the wave equation analysis to obtain the resistance that can be overcome by the hammer-pile-soil system or the analysis to estimate the resistance that the soil will offer to driving. Because of this, considerable engineering judgment must be used with these results to obtain an evaluation of pile drivability. It usually is possible to select a penetration where it is almost certain a pile can be driven and also to select a penetration beyond which a pile probably cannot be driven. This leaves a range of penetration, which may be significantly large, where the actual penetration to which the pile can be driven may depend on factors that cannot be predetermined. However, the results of the drivability analysis used with engineering judgment will permit a better evaluation of the probability of installing a pile to a given penetration with a particular hammer than with no information at all. This information also has been found to be useful to evaluate the effects of unforseen events occurring during pile driving in arriving at decisions that have to be made during pile installation.

REFERENCES

1. Isaacs, D.V., "Reinforced Concrete Pile Formula," *Transactions of the Institution of Engineers, Australia,* Vol. 12, pp. 312-323 (1931).

2. Glanville, W.H., Grime, G., Fox, E.N., and Davies, W.W., "An Investigation of the Stresses in Reinforced Concrete Piles During Driving," *Technical Paper No. 20,* British Building Research Board, 1938.

3. Smith, E.A.L., "Pile Driving Impact," *Proceedings, Industrial Computation Seminar,* September 1950, International Business Machines Corp., New York, N.Y. (1951).

4. Smith, E.A.L., "Impact and Longitudinal Wave Transmission," *Transactions,* ASME, pp. 963-973, August 1955.

5. Smith, E.A.L., "Pile Driving Analysis by the Wave Equation," *Transactions,* ASCE, Vol. 127, Part I, pp 1145-1171 (1962).

6. Hirsch, T.J., Carr, L. and Lowery, L.L., *Pile Driving Analyses-Wave Equation User's Manual,* TTI Program Implementation Package, Vol. I, II, III and IV, 1976.

7. Goble, G.G. and Rausche, F., *Wave Equation Analysis of Pile Driving,* WEAP Program Implementation Package, Vol. I, II, III and IV 1976.

REFERENCES (continued)

8. Forehand, P.W. and Reese, J.L., Jr., "Prediction of Pile Capacity by the Wave Equation," *Journal, Soil Mechanics and Foundation Division,* ASCE, Vol. 90, No. SM2, pp. 1-25 (1964).

9. Lowery, L.L., Hirsch, T.J., Edwards, T.C., Coyle, H.M., and Sampson, C.H., Jr. *Pile Driving Analysis State of the Art,* Texas Transportation Institute Research Report 33-13, Texas A&M University (1969).

10. Foye, R., Jr., Coyle, H.M., Hirsch, T.J., Bartoskewitz, R.E. and Milberger, L.J. *Wave Equation Analyses of Full-Scale Test Piles Using Measured Field Data,* Texas Transportation Institute Research Report 125-7, Texas A&M University (1972).

11. Hirsch, T.J., Lowery, L.L., Coyle, H.M. and Samson, C.H., Jr., "Pile Driving Analysis by One-Dimensional Wave Theory: State of the Art," *Highway Research Record No. 333,* Highway Research Board, pp. 33-54 (1970).

12. Roussel, H.J., Jr., *Pile Driving Analysis of Large Diameter High Capacity Offshore Piles,* Ph.D. Dissertation, Department of Civil Engineering, Tulane University (1979).

13. Heerema, E.P., "Relationships Between Wall Friction, Displacement Velocity and Horizontal Stress in Clay and in Sand, for Pile Drivebility Analysis," *Ground Engineering,* Vol. 12, No. 1, pp. 55-61, 65 (1979).

REFERENCES (continued)

14. American Petroleum Institute, *Recommended Practice for Planning, Designing, and Constructing Fixed Offshore Platforms,* API RP 2A, 12th edition (1981).

15. Vijayvergiya, V.N. and Focht, J.A., Jr., "A New Way to Predict the Capacity of Piles in Clay," *Offshore Technology Conference,* (1972), Vol. 2, pp. 865-874.

16. Vesic, A.S., *Principles of Pile Foundation Design,* Soil Mechanics Series No. 38, School of Engineering, Duke University, (1975).

17. Heerema, E.P., "Predicting Pile Drivability: Heather as an Illustration of the "Friction Fatigue" Theory," *Proceedings, European Offshore Petroleum Conference and Exhibition,* Vol. 1, pp 413-422 (1978).

TABLE 23.1 PROPERTIES OF SOME HAMMERS USED OFFSHORE[1]

Hammer	Rated Energy ft-lb	Weight Ram lb	Weight Impact Block lb	[2]Weight Drive Cap lb	[3]Explosive Force lb
Vulcan 6300	1,800.000	300,000	-	139,285	-
HBM 4000	1,700,000	205,000	-	-	-
Menck 12500	1,582,220	275,580	-	154,320	-
HBM 3000A	1,100,000	152,000	-	-	-
Menck 8000	867,960	176,370	-	97,000	-
Vulcan 5150	750,000	150,000	-	75,000	-
Menck 7000	632,885	154,000	-	92,400	-
HBM 3000	542,471	138,890	-	30,864	-
Vulcan 5100	500,000	100,000	-	-	-
Menck 4600	499,070	101,410	-	61,730	-
HBM 1500	410,000	55,000	-	-	-
Menck 3000	325,480	66,140	-	33,070	-
Vulcan 3100	300,000	100,000	-	-	-
Vulcan 560	300,000	62.500	-	43,100	-
Kobe K-150	289,000	33,100	-	-	639,000
Delmag D80-12	225,000	19,500	-	-	-
Vulcan 540	200,000	40,000	-	32,800	-
Menck 1800	189,850	38,580	-	22,050	-
Vulcan 360	180,000	60,000	-	42,600	-
MKT OS-60	180,000	60,000	-	20,000	-
Delmag D62-02	162,000	14,000	2,420	-	550,000
Mitsubishi MB 70	155,500	15,840	-	-	440,000
Vulcan 530	150,000	30,000	-	10,000	-
MKT OS-40	120,000	40,000	-	-	-
Vulcan 340	120,000	40,000	-	31,300	-
Delmag D55	117,000	12,100	2,420	-	550,000
Kobe K-60	116,000	13,200	-	-	543,000
Vulcan 400C	113,478	40,000	-	31,300	-
Delmag D46-02	105,000	10,120	1,950	-	396,000
Kobe K-45	97.600	9,900	-	-	421,000
Menck 850	93,340	18,960	-	11,660	-
Vulcan 030	90,000	30,000	-	10,000	-
Delmag D44	87,000	9,500	2,420	-	440,000
Delmag D36-02	83,000	7,900	1,980	-	396,900
Kobe K-42	79,600	9,200	-	8,127	-
HBM 500	72,239	9,480	-	-	-
Delmag D30-02	62,900	6,600	1,230	-	277,800
Vulcan 020	60,000	20,000	-	10,000	-
MKT OS-20	60,000	20,000	-	-	-

[1]Information taken from manufacturer's published data.

[2]Offshore drive cap obtained from manufacturer when available; other drive caps may be used.

[3]Maximum explosive force on pile.

TABLE 23.2 - TYPICAL PROPERTIES FOR COMMONLY-USED CAPBLOCK CUSHION MATERIALS

Material	Dynamic Modulus of Elasticity[1] kips/in.^{2}	Coefficient of Restitution
Aluminum Plates	10,300	0.8[2]
Asbestos	150	0.5
Ascon	150	0.6
Conbest	500	0.8
Hardwood (load parallel to grain)	275	0.7
Micarta	450	0.8
Steel Plates	29,600	0.8[2]
Wire Rope Coils	150	0.3

[1] Values for well-compressed, used material and the shear levels of offshore pile driving.

[2] When these metal plates are used in combination with another cushion material the coefficient of restitution of the other material should be used.

TABLE 23.3 HISTORICAL SUMMARY OF QUAKE AND DAMPING VALUES

Parameters		References	Smith 1962	Forehand and Reese, 1964	Lowrey, et al 1969	Foye, et al 1972	Hirsch, et al 1976	Roussel 1979
	Quake in.	Side	0.1	0.05 - 0.15	0.1	0.1	0.1	0.1
		Tip	0.1	0.05 - 0.15	0.1	0.1	0.1	0.1
	Damping sec/ft	Side	0.05	0.017 - 0.067	0.033	0.3 - 0.6 (0.5)	0.05	0.08
		Tip	0.15	0.05 - 0.2	0.1	0	0.15	0.15
Clays	Quake in.	Side	0.1	0.1 - 0.2	0.1	0.1	0.1	0.1 - 0.2
		Tip	0.1	0.1 - 0.2	0.1	0.1	0.1	0.1 - 0.2
	Damping sec/ft	Side	0.05	1/3 of tip damping	0.1	0.1 - 0.3 (0.2)	0.2	0.03 - 0.11
		Tip	0.15	at Quake 0.1: 0.5 - 1.0 at Quake 0.2: 0.3 - 0.5	0.3	0	0.01	0.20 - 0.15

Chapter 22 Illustration Captions

Fig. 23-1	One dimensional wave equation
Fig. 23-2	Hammer-pile-soil system representation
Fig. 23-3	Bearing graphs from wave equation analyses
Fig. 23-4	Force-deformation properties of capblock
Fig. 23-5	Soil load-deformation characteristics
Fig. 23-6	Pile capacity gain with time for steel piles in cohesive soils
Fig. 23-7	Strength loss by remolding for normally-consolidated clays
Fig. 23-8	Pile capacity gain with set-up.
Fig. 23-9	Interpretation of pile driveability - resistance to driving procedure, Example 1
Fig. 23-10	Interpretation of pile driveability - resistance to driving procedure, Example 2
Fig. 23-11	Interpretation of pile driveability - rate of penetration procedure

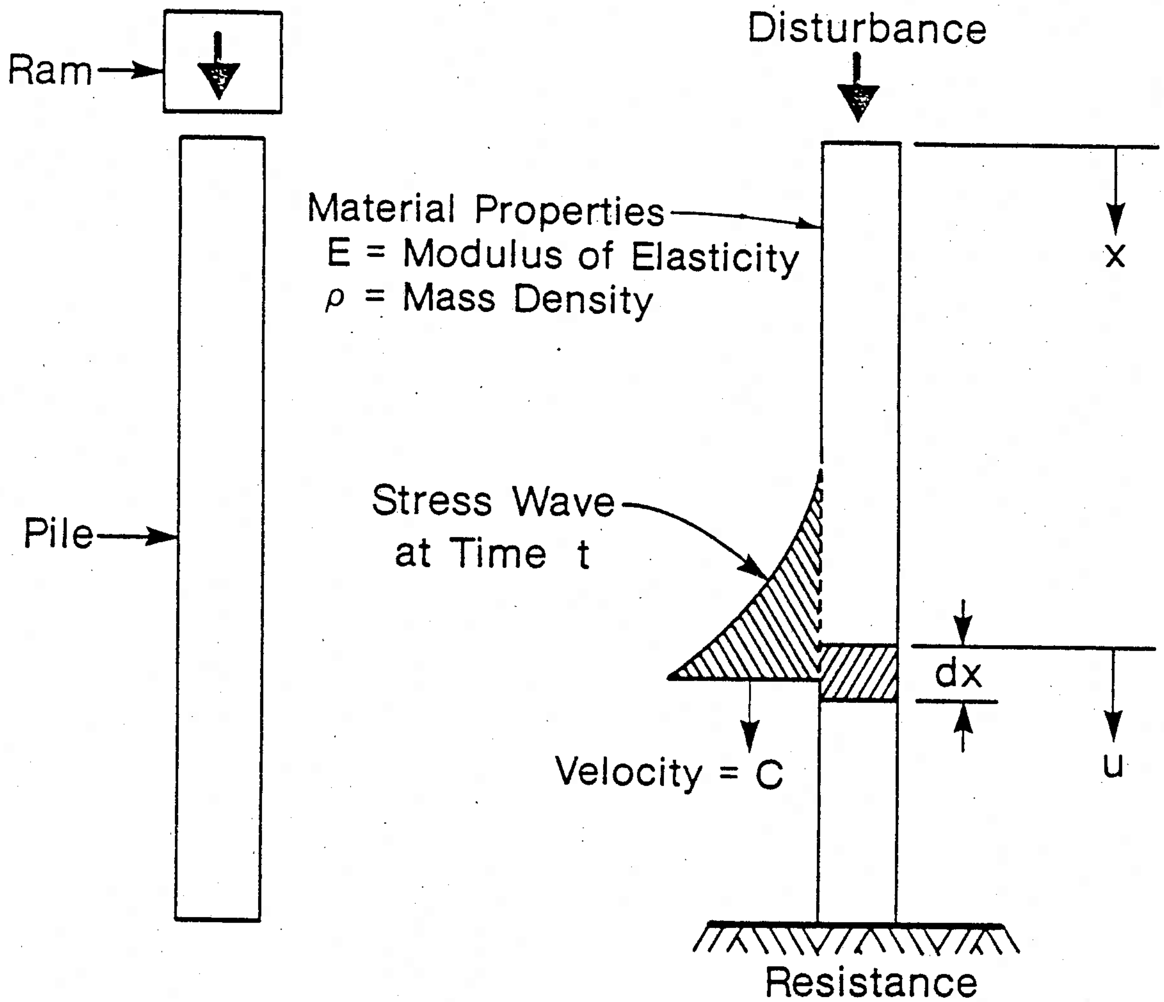

(a)

$$\frac{\partial^2 u}{\partial t^2} = C^2 \frac{\partial^2 \mu}{\partial x^2}$$

$C = \sqrt{E/\rho}$ = Stress Wave Velocity

(b)

(Fig 23-1)

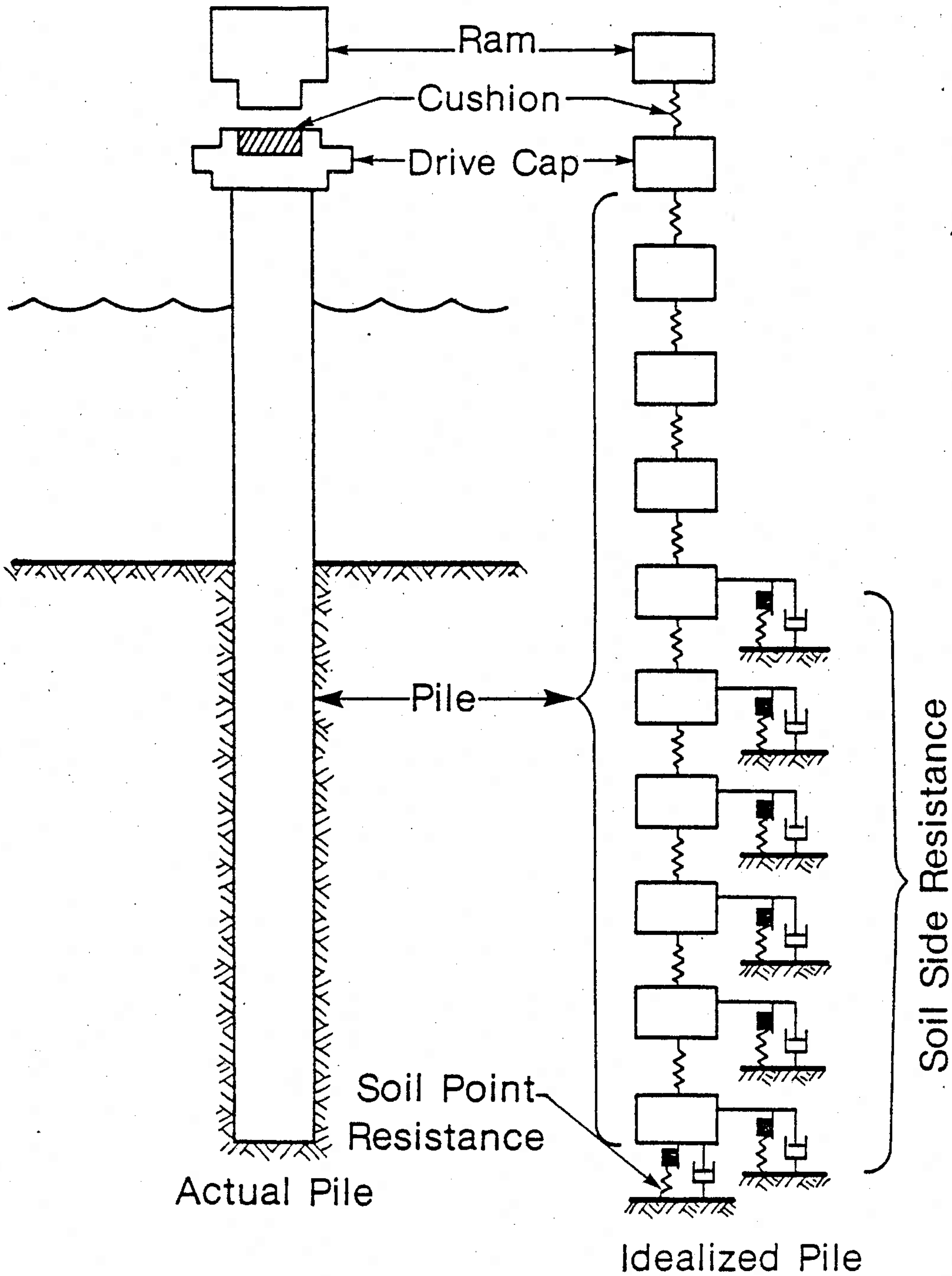
Ram
Cushion
Drive Cap
Pile
Soil Side Resistance
Soil Point Resistance
Actual Pile
Idealized Pile

(Fig 23-2)

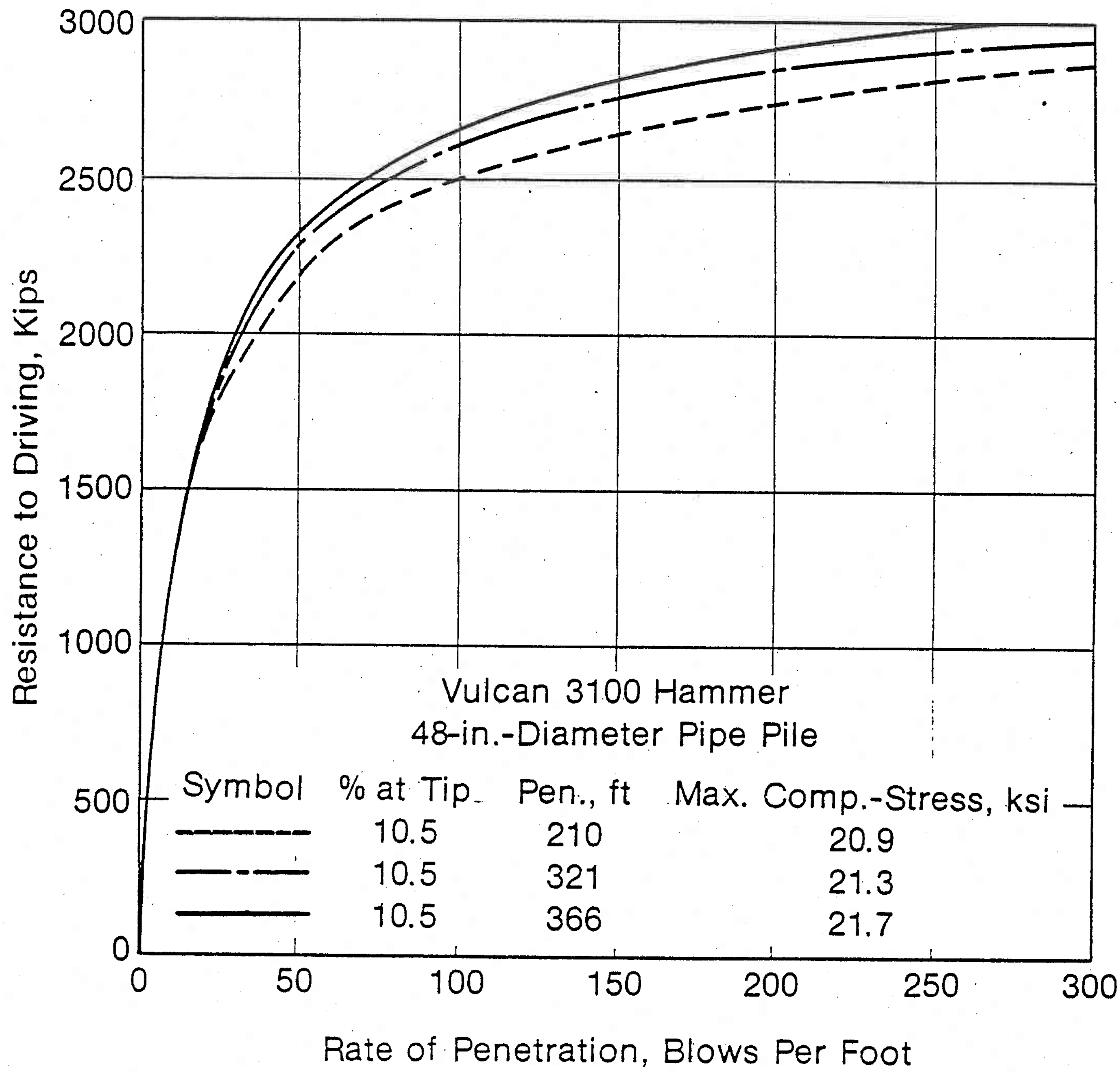
Resistance to Driving, Kips
3000
2500
2000
1500
1000
500
0
0
50
100
150
200
250
300
Rate of Penetration, Blows Per Foot
Vulcan 3100 Hammer
48-in.-Diameter Pipe Pile
Symbol
% at Tip
Pen., ft
Max. Comp.-Stress, ksi
10.5
210
20.9
10.5
321
21.3
10.5
366
21.7

(Fig 23-3)

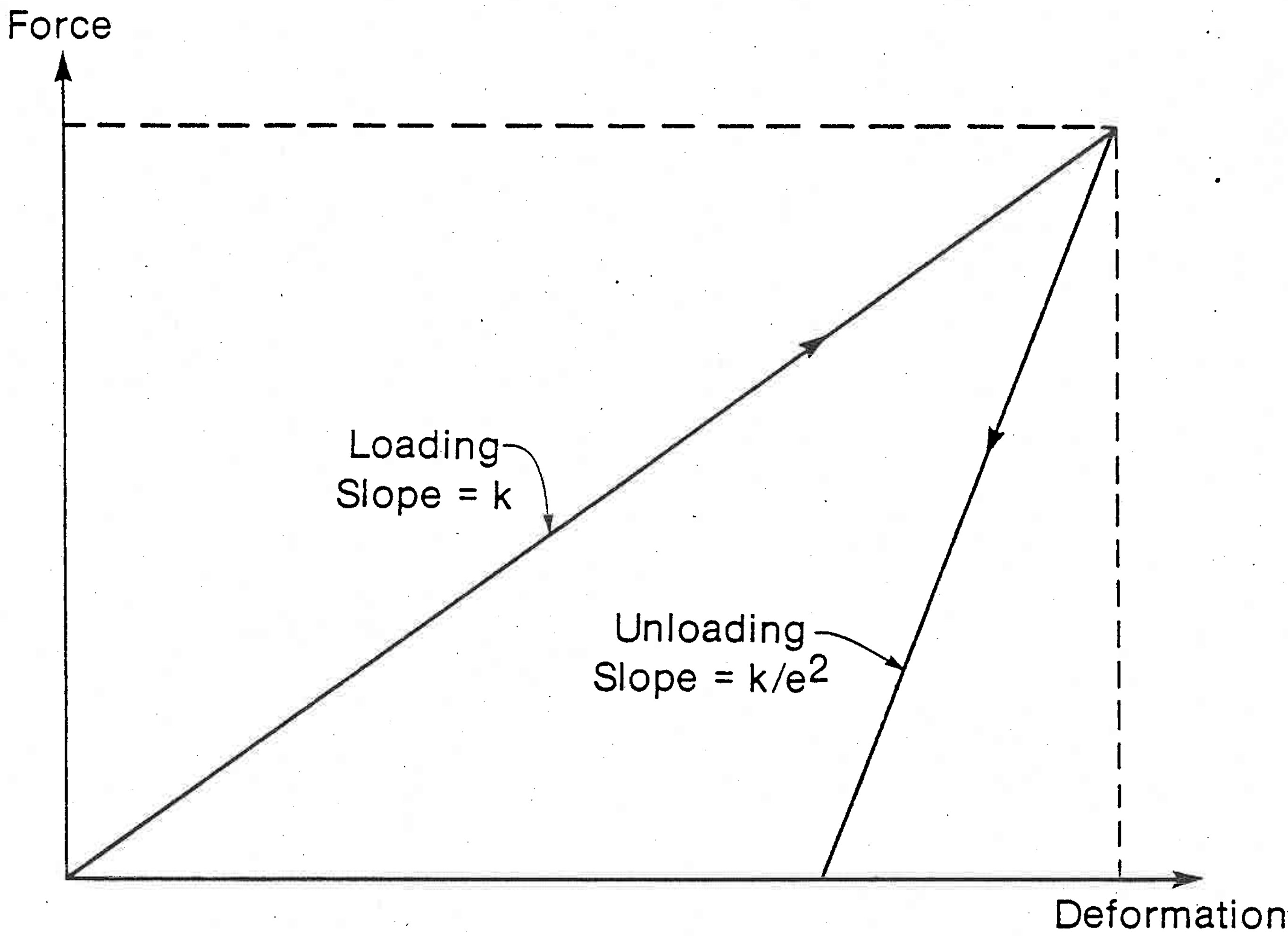

(Fig 23-4)

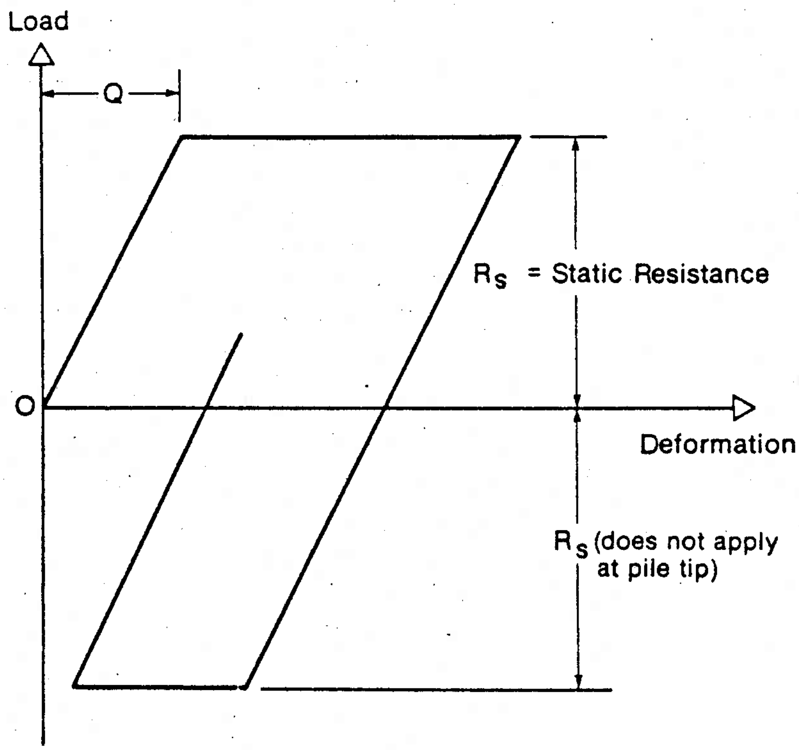

(a) Static

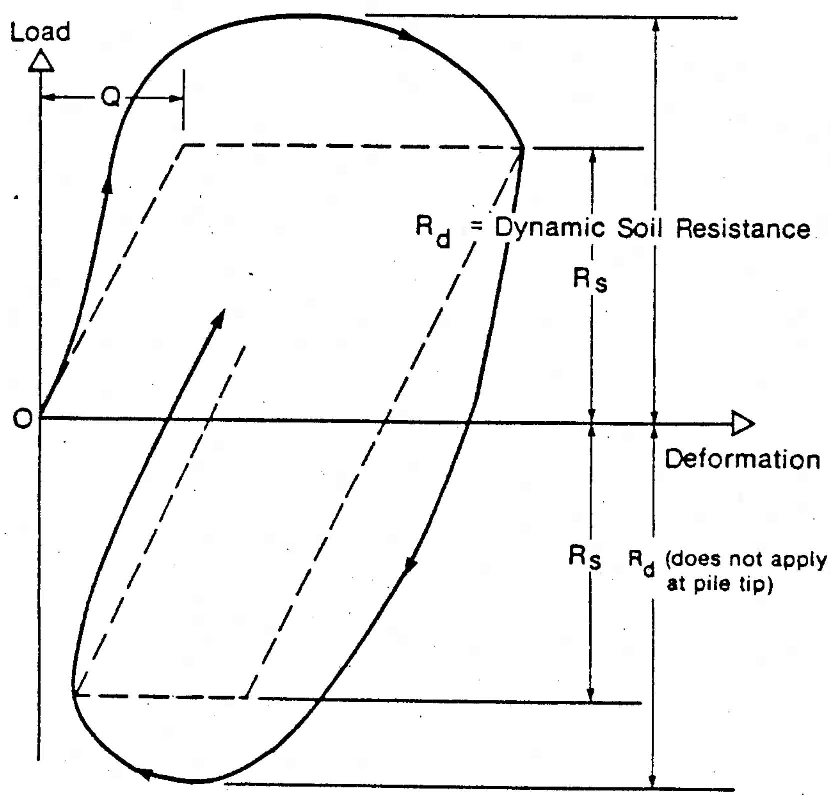

(b) Dynamic

(After Hirsch, et. al. 1970)

(Fig 23-5)

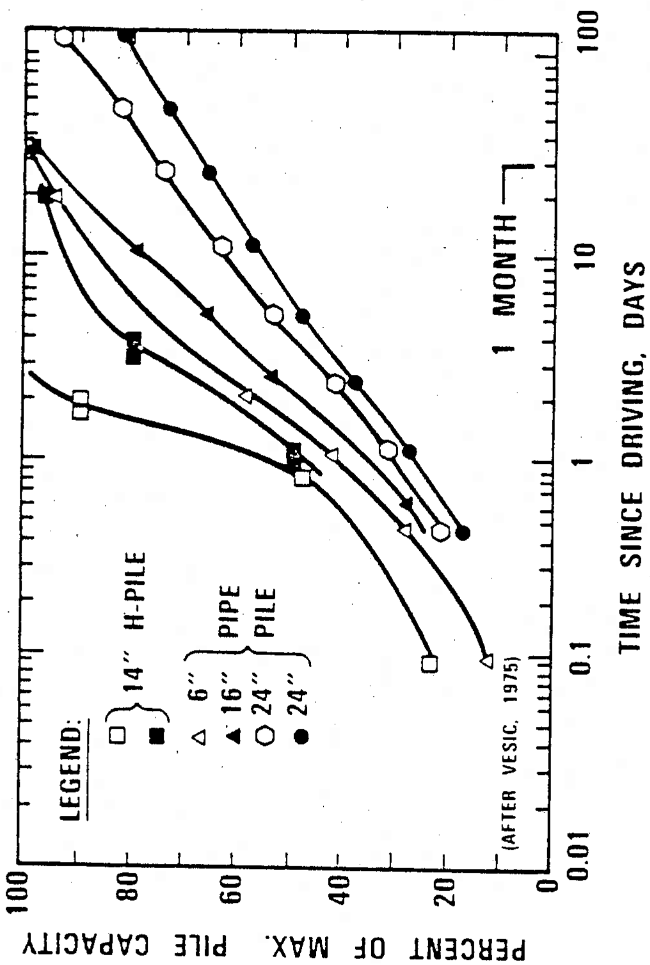

LEGEND:
14" H-PILE
6"
16"
24"
24"
PIPE PILE
(AFTER VESIC, 1975)
1 MONTH
PERCENT OF MAX. PILE CAPACITY
100
80
60
40
20
0
0.01
0.1
1
10
100
TIME SINCE DRIVING, DAYS

(Fig 23-6)

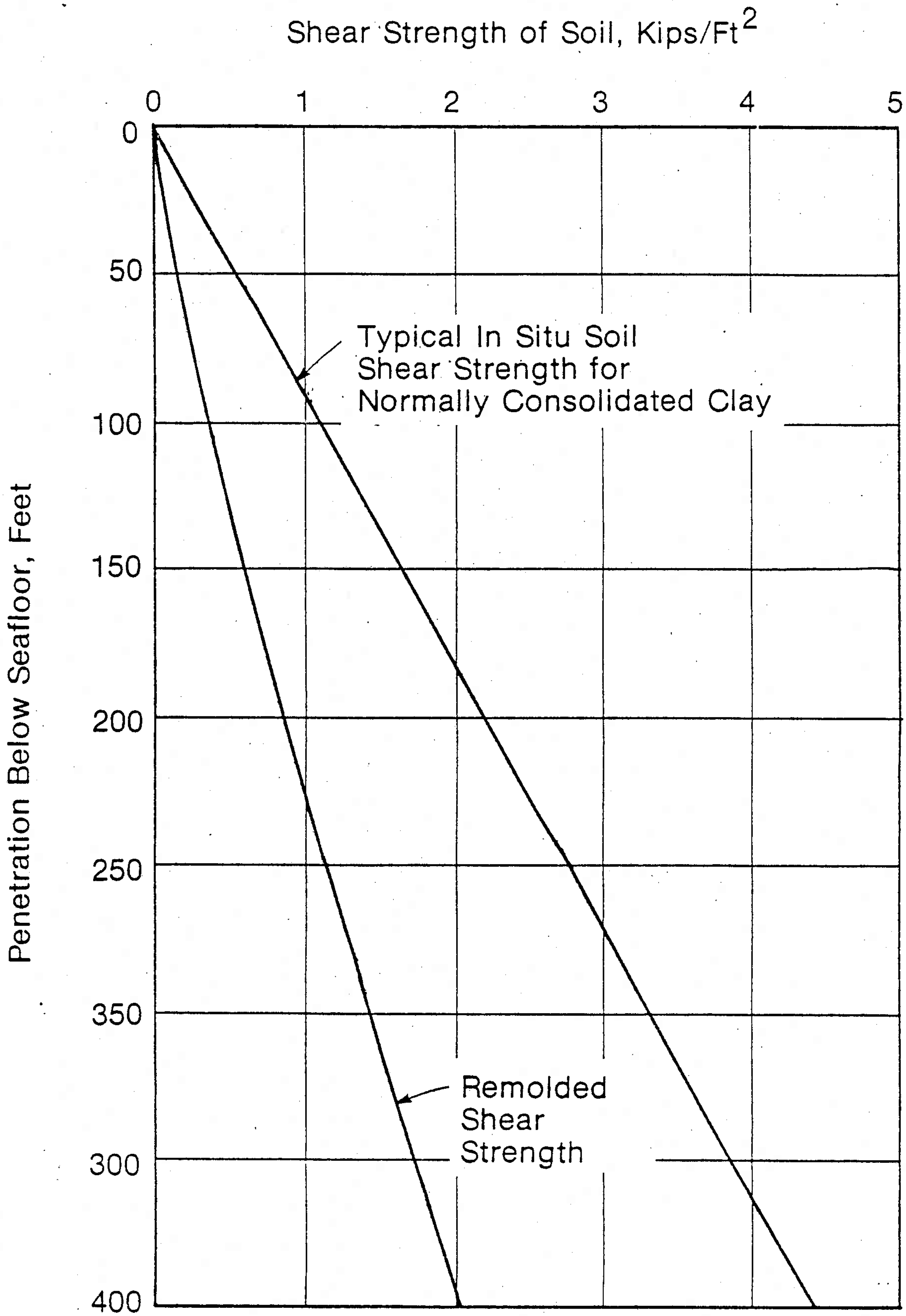
Shear Strength of Soil, Kips/Ft^2
0
1
2
3
4
5
0
50
100
150
200
250
350
300
400
Penetration Below Seafloor, Feet
Typical In Situ Soil Shear Strength for Normally Consolidated Clay
Remolded Shear Strength

(Fig 23-7)

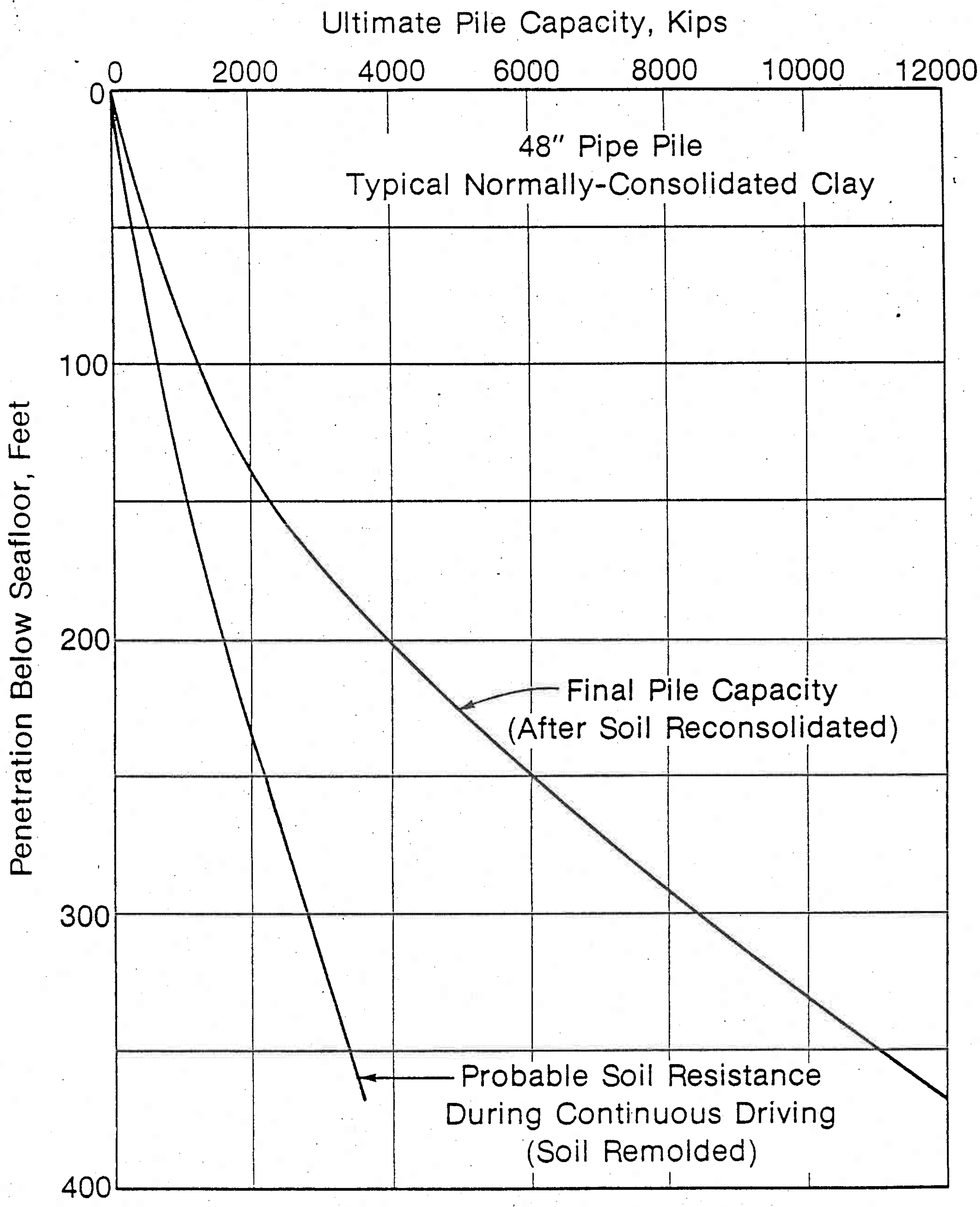
Ultimate Pile Capacity, Kips
0
2000
4000
6000
8000
10000
12000
0
100
200
300
400
Penetration Below Seafloor, Feet
48" Pipe Pile
Typical Normally-Consolidated Clay
Final Pile Capacity
(After Soil Reconsolidated)
Probable Soil Resistance
During Continuous Driving
(Soil Remolded)

(Fig. 23-8)

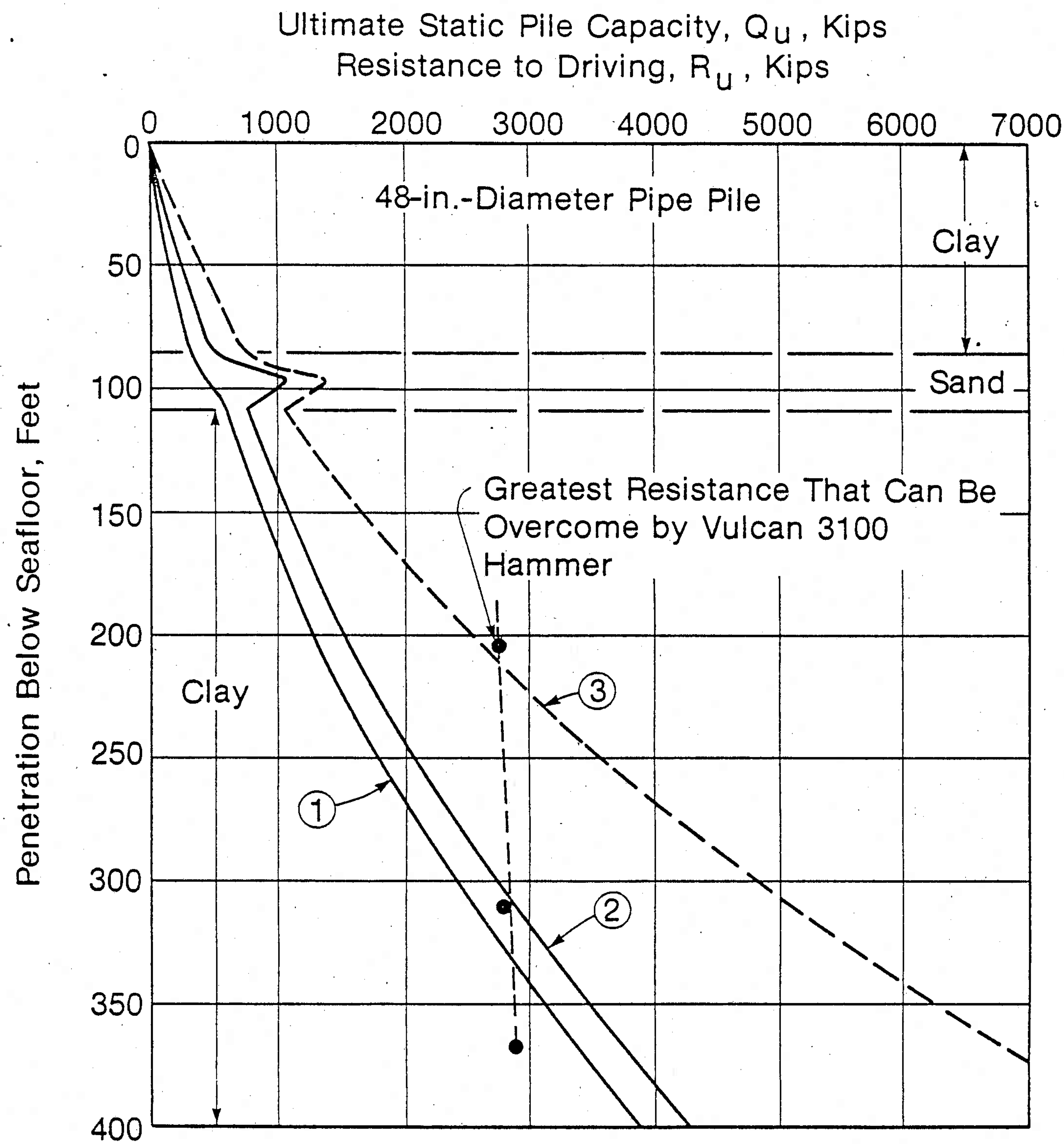

1. Estimated Resistance to Driving, R_u , based on remolded side friction in clay, static side friction in sand and end bearing on pile wall end area.
2. Estimated Resistance to Driving, R_u , based on remolded side friction in clay, static side friction in sand and end bearing on pile gross end area.
3. Computed Ultimate Compressive Pile Capacity, Q_u

(Fig 23-9)

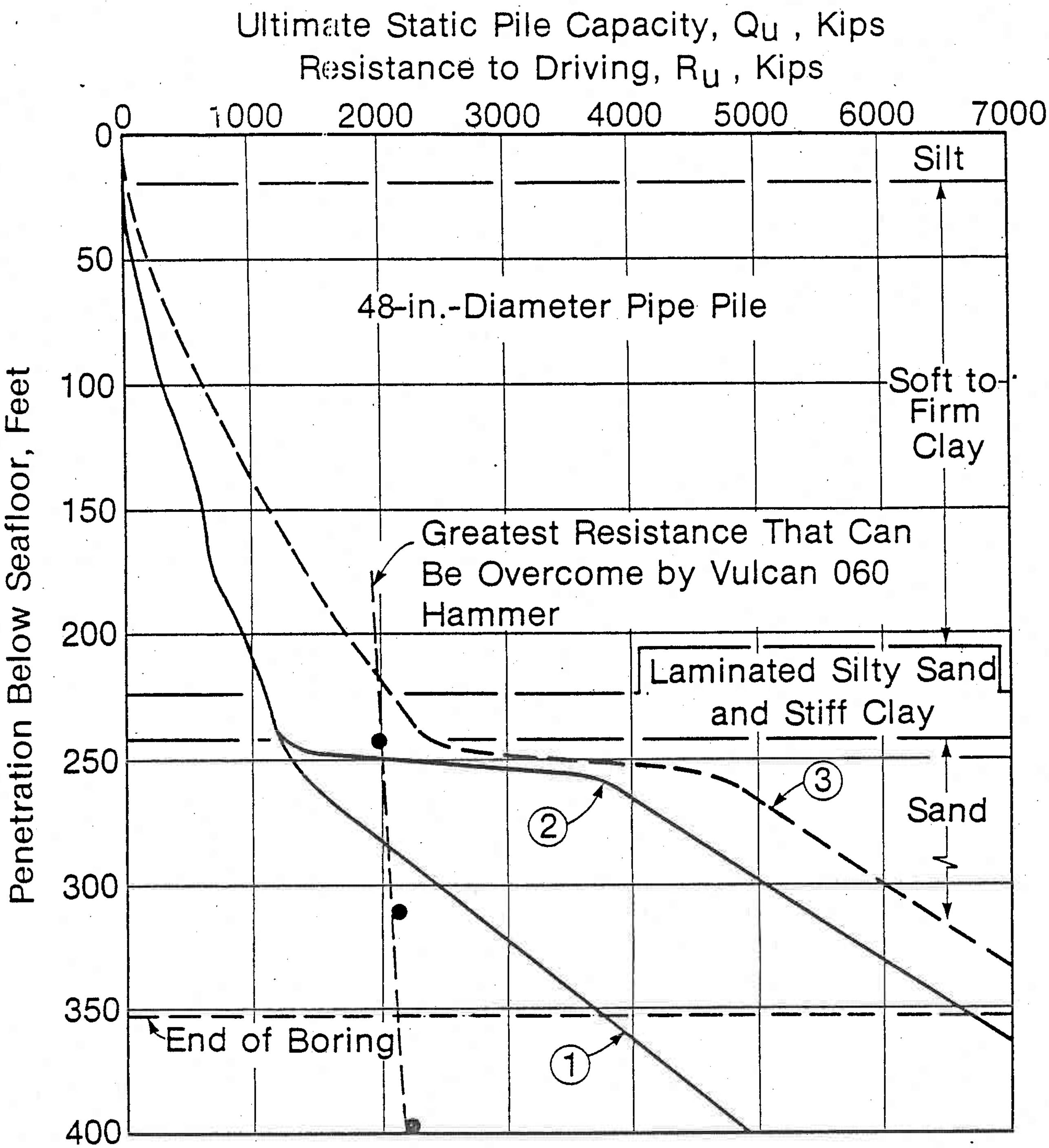

1. Estimated Resistance to Driving, R_u, based on remolded side friction in clay, static side friction in sand and end bearing on pile wall end area.
2. Estimated Resistance to Driving, R_u, based on remolded side friction in clay, static side friction in sand and end bearing on pile gross end area.
3. Computed Ultimate Compressive Pile Capacity, Q_u

(Fig 23-10)